

The Hamburg/SAO survey for emission–line galaxies

VI. The sixth list of 126 galaxies

S.A. Pustilnik¹, D. Engels², V.A. Lipovetsky^{1,*}, A.Y. Kniazev^{1,3}, A.G. Pramskij¹, A.V. Ugryumov¹,
J. Masegosa⁴, Y.I. Izotov⁵, F. Chaffee⁶, I. Márquez⁴, A.L. Teplyakova⁷,
U. Hopp⁸, N. Brosch⁹, H.-J. Hagen², and J.-M. Martin¹⁰

¹ Special Astrophysical Observatory, Nizhnij Arkhyz, Karachai-Circassia, 369167, Russia

² Hamburger Sternwarte, Gojenbergsweg 112, D-21029 Hamburg, Germany

³ European Southern Observatory, Karl-Schwarzschild-Strasse 2, 85748 Garching, Germany

⁴ Instituto de Astrofísica de Andalucía, CSIC, Aptdo. 3004, 18080, Granada, Spain

⁵ Main Astronomical Observatory, 27 Zabolotnoho str., Kyiv, 03680, Ukraine

⁶ Keck Observatories, Hawaii, USA

⁷ Sternberg Astronomical Institute, Moscow State University, Moscow

⁸ Universitätssternwarte München, Scheiner Str. 1, D-81679 München, Germany

⁹ Wise Observatory, Tel-Aviv University, Tel-Aviv 69978, Israel

¹⁰ GEPI, Observatoire de Paris, F-92195 Meudon Cedex, France

Received 1 December 2004; Accepted 15 June 2005

Abstract. We present the sixth list with results** of the Hamburg/SAO Survey for Emission-Line Galaxies. The final list resulted from follow-up spectroscopy conducted with the 4.5 m MMT telescope in 1996, and with 2.2 m CAHA and 6 m SAO telescopes in 2000 to 2003. The data of this snap-shot spectroscopy survey confirmed 134 emission-line objects out of 182 observed candidates and allowed their quantitative spectral classification and redshift determination. We classify 73 emission-line objects as definite or probable blue compact or HII galaxies (BCG), 8 as QSOs, 4 as Seyfert 1 and 2 galaxies. 30 low-excitation objects were classified as definite or probable starburst nuclei (SBN), 3 as dwarf amorphous nuclei starburst galaxies (DANS) and 2 as LINERs. Due to the low signal-to-noise ratio we could not classify 14 ELGs (NON). For another 9 galaxies we did not detect any significant emission lines. For 98 emission-line galaxies, the redshifts and/or line intensities are determined for the first time. For the remaining 28 previously-known ELGs we give either improved data the line intensities or some independent measurements. The detection rate of ELGs is ~70%. This paper completes the classification of strong-lined ELGs found in the zone of the Hamburg/SAO survey. Together with previously known BCG/HII galaxies in this zone, this sample of ~500 objects is the largest to date in a well bound region.

Key words. surveys – galaxies: fundamental parameters – galaxies: distances and redshifts – galaxies: starburst – galaxies: compact – quasars: redshifts

1. Introduction

The problem of creating large, homogeneous and deep samples of actively star-forming low-mass galaxies is very important for several applications in studies of galaxy evolution and spatial distribution. Several earlier projects, based on objective prism plates, like the Second Byurakan

Survey (SBS) (Markarian et al. 1983, Stepanian 1994), the University of Michigan (UM) survey (e.g., Salzer et al. 1989) and the Case survey (Pesch et al. 1995, Salzer et al. 1995, Ugryumov et al. 1998), as well as some others (e.g., Kitt Peak International Spectral Survey – KISS, Salzer et al. 2000, based on CCD detector registration) identified several thousand emission-line galaxies. The Hamburg/SAO survey (HSS) creates a new very large homogeneous sample of such galaxies in the region of the Northern sky with an area of some 1700 square degrees. It was initiated, in particular, in order to close the gap between the sky regions of the SBS and the original Case survey, and as a result to get the combined sample of low-

Send offprint requests to: S. Pustilnik e-mail: sap@sao.ru

* Deceased 1996 September 22.

** Tables 4 to 8 are only available in electronic form at the CDS via anonymous ftp to [cdsarc.u-strasbg.fr](ftp://cdsarc.u-strasbg.fr) (130.79.128.5) or via <http://cdsweb.u-strasbg.fr/Abstract.html>. Figures A1 to A13 will be made available only in the electronic version of the journal.

Table 1. Journal of observations

Date	Telescope	Instrument	Grating, grism	Wavelength range [Å]	Dispersion [Å/pixel]	Observed number
(1)	(2)	(3)	(4)	(5)	(6)	(7)
20.05.1996	4.5 m MMT	MMT Spect	R300	3700–7400	3.2	42
11-12.04.2000	6 m BTA	LSS	R325	3600–7600	4.6	24
25.05.2000	6 m BTA	LSS	R325	3600–7600	4.6	1
28.06-04.07.2000	2.2 m CAHA	CAFOS	G-200	3700–9500	4.5	54
03.10-31.10.2000	6 m BTA	LSS	R651	3700–6000	2.3	5
17.01-20.01.2001	6 m BTA	LSS	R651	3700–6000	2.3	16
16-19.02.2002	6 m BTA	LSS	R400	3700–7600	3.8	15
14-15.02.2002	2.2 m CAHA	CAFOS	G-200	3700–9500	4.5	14
10.12-13.12.2002	6 m BTA	LSS	R400	3700–7600	3.8	10
24.12.2003	6 m BTA	LSS	R400	3700–7600	3.8	4

Table 2. Summary of the samples observed and breakdown of the classifications after follow-up spectroscopy

Candidate Sample		N	BCG & BCG?	Other ELGs	QSO	Galaxies without emission	Stars	Not Classified
First priority	new	36	21	8	1	1	4	1
	already known	40	31	9	–	–	–	–
	total	76	52	17	1	1	4	1
Second priority	new	77	11	17	6	8	22	12
	already known	29	9	20	1	–	–	–
	total	106	20	37	7	8	22	12
Objects presented in this paper		182	72	54	8	9	26	13

mass emission-line galaxies in a very large section of sky suitable for the study of their spatial distribution.

The basic outline of the HSS and its first results are described in Paper I (Ugryumov et al. 1999), while the additional results from the follow-up spectroscopy are given in papers II, III, IV and V (Pustilnik et al. 1999, Hopp et al. 2000, Kniazev et al. 2001, Ugryumov et al. 2001). In this, the last paper, we present the results of the follow-up spectroscopy of another 182 objects selected on the Hamburg Quasar Survey (HQS) prism spectral plates as ELG candidates. In Table 2 we show the breakdown of these objects in the samples of the 1st and 2nd priority group, and the categories of detected objects as described below. Out of 134 emission-line objects (galaxies and QSOs) 69 were known as NED objects. For 28 of these galaxies either only redshift, or also some information on emission lines was known, mainly from the previous HSS papers. We included such objects in the presented list since we provide either significantly improved data or some independent measurements.

The article is organized as follows. In section 2 we give the details of the spectroscopic observations and of the data reduction. In section 3 the results of the observations are presented in several tables. In section 4 we briefly discuss the new data and summarize the current state of the

Hamburg/SAO survey. Throughout this paper a Hubble constant $H_0 = 75 \text{ km s}^{-1} \text{ Mpc}^{-1}$ is used.

2. Spectral observations and data reduction

2.1. Observations

The results presented here were obtained mostly in snapshot observing mode during one run with the 4.5 m Multiple Mirror Telescope (MMT), two runs with the Calar Alto 2.2 m and seven runs with the SAO 6 m (BTA) telescopes (see Table 1).

2.2. Observations with the MMT 4.5 m telescope

The observations were carried out on May 20, 1996, with the Red Channel of the MMT Spectrograph through the long slit of $1''5 \times 180''$. The 300 grooves mm^{-1} grating in first order provides a dispersion of 3.2 Å pixel^{-1} , and a spectral resolution FWHM of about 10 Å . To avoid second-order contamination, a L-38 blocking filter was used. The total spectral range was $\lambda\lambda 3700\text{--}7400 \text{ Å}$. The spectra were rebinned by a factor of 2 along the spatial axis. Hence, the spatial sampling was $0''.6 \text{ pixel}^{-1}$.

Short exposures (3–5 minutes) were taken in order to detect strong emission lines to allow redshift measurements and a crude classification. The slit was not oriented along the parallactic angle because of the snapshot observing mode. Reference spectra of an Ar–Ne–He lamp were recorded to provide wavelength calibration. Spectrophotometric standard stars from Oke (1990) and Bohlin (1996) were observed at the beginning and at the end of the night for flux calibration. The dome flats, bias, dark and twilight sky frames were accumulated each night. The weather conditions were photometric, with seeing variations around $1''.0$ (FWHM).

2.3. Calar Alto 2.2 m telescope observations

Follow-up spectroscopy with the CAHA 2.2 m telescope was carried out during two runs (June–July 2000 and February 2002), using the Calar Alto Faint Object Spectrograph (CAFOS). During these runs a long slit of $300'' \times 2''$ and a G-200 grism (187 \AA mm^{-1} , first order) were used. The spatial scale along the slit was $0''.53 \text{ pixel}^{-1}$. A SITE 15 2K \times 2K CCD was operated without binning. The wavelength coverage was $\lambda 3700 - \lambda 9500 \text{ \AA}$ with maximum sensitivity at $\sim 6000 \text{ \AA}$. The spectral resolution was $\sim 12\text{--}16 \text{ \AA}$ (FWHM). The slit orientation was not aligned with the parallactic angle because of the snapshot observing mode. The exposure times varied within 5 – 20 minutes depending on the object brightness and weather conditions. The observations were complemented by standard star flux measurements (Oke 1990, Bohlin 1996), reference spectra (Hg–Cd lamp) for wavelength calibration, dome flat, bias and dark frames. In the run of June–July 2000 the weather conditions were photometric most of the time with a seeing $\approx 1.5''$ (FWHM). During one night of this run, as well as during two nights in February 2002, the weather conditions were variable with a seeing of $3'' - 4''$. The measurements in these nights are marked by “*” in Table 5.

There was no order separation filter applied, therefore some second order contamination by the object UV light might be present at wavelengths longer than 7200 \AA . However, as can be directly seen from the presented spectra, this effect is probably small, since it is undetectable in the continuum behavior around $\lambda 7200 \text{ \AA}$. In principle, one could expect an increase of the line fluxes at wavelengths longer than this due to the second order contamination in the spectra of the flux calibrating stars. There are seven objects whose emission line ratios could be potentially affected. These objects are listed and commented at the end of section 3.1.

2.4. BTA 6 m telescope observations

The observations with the 6 m telescope (BTA) of the Special Astrophysical Observatory of Russian Academy of Sciences (SAO RAS) were performed mainly as a backup program. Therefore the weather conditions in most

cases were rather poor. The seeing in the majority of the nights was in the range of $2''$ to $4''$ (FWHM) and/or the transparency was variable. Results obtained under non-photometric conditions are marked by “*” in Table 5. In all cases we used the long slit spectrograph (LSS) in the BTA prime focus (Afanasiev et al. 1995) with a Photometrics 1K \times 1K CCD detector with $24 \mu\text{m}$ pixel size. The long slit of $120''$ was used with the slit width of either $1''.5$ or $2''.0$, depending on the seeing and grating. Three set-ups with the gratings of 325, 400 and $651 \text{ grooves mm}^{-1}$ were used during various runs. The wavelength ranges of the spectra covered for different set-ups and their samplings in \AA pixel^{-1} are given in Table 1. The respective effective resolutions were $\sim 14 \text{ \AA}$, $\sim 11 \text{ \AA}$ and $\sim 7 \text{ \AA}$.

Reference spectra of an Ar–Ne–He lamp were recorded before or after each observation to provide wavelength calibration. Spectrophotometric standard stars from Bohlin (1996) were observed for flux calibration. All observations were conducted mainly with the software package NICE in MIDAS, described by Kniazev & Shergin (1995).

2.5. Data reduction

The reduction of all data was performed at SAO using the standard reduction systems MIDAS¹ and IRAF².

The MIDAS command FILTER/COSMIC was found to be a quite successful way to automatically remove all cosmic ray hits from the images. After that we applied the IRAF package CCDRED for bad pixel removal, trimming, bias-dark subtraction, slit profile and flat-field corrections.

To do accurate wavelength calibration, correction for distortion and tilt for each frame, sky subtraction and correction for atmospheric extinction, the IRAF package LONGSLIT was used.

To obtain an instrumental response function from observed spectrophotometric flux standards, we first extracted the apertures of standard stars. Then the determined sensitivity curve was applied to perform flux calibration for all object images. Finally we extracted one-dimensional spectra from the flux calibrated images. When more than one exposure was taken with the same setup for a given object, the extracted spectra were co-added and a mean vector was calculated. When several observations with different setups (telescopes or gratings) for the same object were obtained, the data were reduced and measured independently and the more accurate values were taken.

To speed-up and facilitate the line measurements we employed the dedicated command files created at SAO using the FIT context and MIDAS command language. The procedures for the measurements of line parameters and

¹ MIDAS is an acronym for the European Southern Observatory package – Munich Image Data Analysis System.

² IRAF is distributed by National Optical Astronomical Observatory, which is operated by the Association of Universities for Research in Astronomy, Inc., under cooperative agreement with the National Science Foundation

redshifts applied were also described in detail in Papers III, IV and in Kniazev et al. (2004).

3. Results of follow-up spectroscopy

In Table 2 we present the summary of the observation results. 182 candidates were selected from our first and second priority samples introduced in Paper IV.

Out of 76 first priority candidates (objects showing a clear density peak near $\lambda 5000 \text{ \AA}$ and a blue continuum on the HQS prism spectral plates), 36 objects appeared in our list as new ones. 40 objects were listed in the NED as galaxies or objects from various catalogs and 4 of them already had information on emission lines and redshifts in earlier publications. Apart from these 4 objects, 24 more of the mentioned 40 NED galaxies have appeared in our previous HSS papers, but had data of rather low quality. All such objects were included in our observing program in order to improve spectral information. The comparison of our measured velocities with those of galaxies with already known redshift shows acceptable consistency for most objects in common within the uncertainties given. However, for five galaxies originally appearing in the HSS List II, the difference found is as high as $200\text{--}300 \text{ km s}^{-1}$, which probably indicates the lower accuracy of some radial velocities from that list.

The remaining 106 observed objects were taken from the list of the second priority candidates, those with less prominent emission features on the high resolution spectra (HRS) obtained after scanning the original HQS objective prism plates. As described in Paper IV, we created from this list the “APM selected sample”, which uses additional information for the selection. The “APM selected” sample comprises second priority candidates which are classified as non-stellar (at least in one of two filters) on Palomar Sky Survey plates (PSS) in the APM database, and have a blue colour according to the APM colour system ($(B - R)_{\text{APM}} < 1.0$). Here we give the spectral data for 64 of them, that looked like ELGs or QSOs. 31 more 2nd priority candidates were classified as stars or galaxies without emission, and 12 objects with no emission lines were not classified at all due to poor S/N ratio spectra.

3.1. Emission-line galaxies

The parameters of the 126 observed emission line galaxies are listed in Table 4, containing the following information:

- column 1:* Number in the Table.
- column 2:* The object’s IAU-type name with the prefix HS.
- column 3:* Right ascension for equinox B1950.
- column 4:* Declination for equinox B1950. The coordinates were measured on direct plates of the HQS and are accurate to $\sim 2''$ (Hagen et al. 1995).
- column 5:* Heliocentric velocity and its r.m.s. uncertainty in km s^{-1} .
- column 6:* Apparent B-magnitude obtained by calibration of the digitized photoplates with photometric standard stars (Engels et al. 1994), having an r.m.s. accuracy of \sim

$0^{\text{m}}5$ for objects fainter than $m_B = 16^{\text{m}}0$ (Popescu et al. 1996). Since the algorithm to calibrate the objective prism spectra is optimized for point sources, the brightnesses of extended galaxies are underestimated. The resulting systematic uncertainties are expected to be as large as 2 mag (Popescu et al. 1996). For about 30% of our objects, B-magnitudes are unavailable at the moment. We present for them blue magnitudes obtained from the APM database. They are marked by a “*” before the value in the corresponding column. According to our estimate they are systematically brighter by $0^{\text{m}}92$ than the B-magnitudes obtained by calibration of the digitized photoplates (r.m.s. $1^{\text{m}}02$).

column 7: Absolute B-magnitude, calculated from the apparent B-magnitude and the heliocentric velocity. No correction for galactic extinction is made because all objects are located at high galactic latitudes and the corrections are significantly smaller than the uncertainties in the magnitudes.

column 8: Preliminary spectral classification type according to the spectral data presented in this article. BCG means a galaxy possessing a characteristic HII-region spectrum with low enough luminosity ($M_B \geq -20^{\text{m}}$). SBN and DANS are galaxies of lower excitation with a corresponding position in the line ratio diagnostic diagrams, as discussed in Paper I. SBN are the brighter fraction of this type. Here we follow the notation of Salzer et al. (1989). The non-confident classification is followed by “?”. Three objects (HS 0807+4103, HS 1525+4344, HS 1627+3625) were recognized as Sy 1 galaxies due to the presence of broad Balmer lines and broad [FeII] emission. HS 1644+3934 was recognized as a Seyfert 2 galaxy. The typical spectrum of low-ionization nuclear emission-line regions (LINERs) is identified for 2 galaxies. 14 ELGs are difficult to classify, mainly due to low S/N. They are coded as NON.

column 9: One or more alternative names, according to the information from NED. References are given to the other sources of the redshift-spectral information indicating that a galaxy is an ELG.

The spectra of all emission-line galaxies are shown in Appendix A, which is available only in the electronic version of the journal.

The results of line flux measurements are given in Table 5 which contains the following information:

- column 1:* Number in the Table.
- column 2:* The object’s IAU-type name with the prefix HS. Asterisks refer to the objects observed during non-photometric conditions.
- column 3:* Designation of the telescope with which the spectral data were obtained. ‘B’ means BTA, ‘C’ - Calar Alto 2.2 m telescope, and ‘M’ - MMT.
- column 4:* Observed flux (in $10^{-16} \text{ erg s}^{-1} \text{ cm}^{-2}$) of the $H\beta$ line. The accuracy of this and other parameters varies substantially over the whole table. We divided the relative errors into four intervals: $\leq 5\%$, $(5\text{--}10)\%$, $(10\text{--}20)\%$ and $(20\text{--}50)\%$. They are marked by the respective superscripts *a*, *b*, *c* and *d* right of each table entree. For

about 40% of ELGs the Balmer absorptions from the underlying stellar population can somewhat affect the measured $H\beta$ emission flux and the related flux ratios. These objects are marked with “†”. For several objects with non-detected $H\beta$ emission line, the fluxes are given for $H\alpha$ and marked by a “‡”.

columns 5,6,7: The observed flux ratios $[OII]/H\beta$, $[OIII]/H\beta$ and $H\alpha/H\beta$.

columns 8,9: The observed flux ratios $[NII] \lambda 6583 \text{ \AA}/H\alpha$, and $([SII] \lambda 6716 \text{ \AA} + \lambda 6731 \text{ \AA})/H\alpha$.

columns 10,11,12: Equivalent widths of the lines $[OII] \lambda 3727 \text{ \AA}$, $H\beta$ and $[OIII] \lambda 5007 \text{ \AA}$.

Below we give comments on some specific cases:

HS 1010+4907 and *HS 1009+4906* comprise a compact group (~ 50 kpc in extent) with a fainter galaxy without evident emission lines, namely *HS 1010+4906* (see Table 7).

HS 1353+4706 was classified as an M-star in Paper I (Ugryumov et al. 1999). However, it was suspected that a wrong object had been observed about 0.3 away. This object will be referred to as *HS 1353+4706A*. The new observations indeed revealed that *HS 1353+4706B* is a very strong-lined BCG with very low metallicity ($12 + \log(O/H) = 7.63 \pm 0.03$; see Pustilnik et al. 2004b). The M-dwarf *HS 1353+4706A* has B1950 coordinates 13 53 25.2 +47 06 46 and its brightness is $B > 18.7$.

Seven galaxies observed with the Calar Alto 2.2 m telescope have $H\alpha$, $[NII]$ or $[SII]$ lines at $\lambda > 7200 \text{ \AA}$. Their fluxes can be affected by the second order contamination as pointed out in Sect. 2.3. For these galaxies (1231+4349, 1235+4108, 1426+3658, 1437+3724, 1439+3704, 1525+4344 and 1614+4450) the affected parameters in Table 5 can be either the ratio $F(H\alpha)/F(H\beta)$, or the line flux $F(H\alpha)$, if $H\beta$ was not detected. For the ratios of $F([NII])/F(H\alpha)$ and $F([SII])/F(H\alpha)$ the effect should be minor since these lines are close in wavelength.

3.2. Quasars

The main criteria applied to search for BCGs are blue continuum near $\lambda 4000 \text{ \AA}$ and a strong emission line, the expected doublet $[OIII] \lambda 4959, 5007 \text{ \AA}$, in the wavelength region between 5000 \AA and the sensitivity break of the Kodak IIIa-J photoemulsion near 5400 \AA (see Paper I). For this reason faint QSOs with $Ly\alpha \lambda 1216 \text{ \AA}$ redshifted to $z \sim 3$, or with $CIV \lambda 1549 \text{ \AA}$ redshifted to $z \sim 1.7$, or with $MgII \lambda 2798 \text{ \AA}$ redshifted to $z \sim 0.8$ could be selected as BCG candidates. In Papers I–V we reported the discovery of a number of such faint QSOs. They were missed by the Hamburg Quasar Survey since it is restricted to bright QSOs ($B \leq 17 - 17.5$). Here we report the discovery of eight faint ($B \geq 17.5$) QSOs. For four of them we identified $Ly\alpha \lambda 1216 \text{ \AA}$ redshifted to $z \sim 3$ as the line responsible for its selection. Two objects (*HS 1608+3546* and *HS 1714+4202*) show a broad emission line tentatively identified as $MgII \lambda 2798 \text{ \AA}$ at $z \sim$

0.83–0.84. Two more quasars with $z \sim 1.7$ were selected due to the line $CIV \lambda 1549 \text{ \AA}$. Since for *HS 1203+3811* only one broad line is seen in a rather poor S/N ratio spectrum, its identification as $Ly\alpha$ should be considered as tentative. The data for all eight quasars are presented in Table 6. Finding charts and plots of their spectra can be found on the www-site of the Hamburg Quasar Survey (<http://www.hs.uni-hamburg.de/hqs.html>).

3.3. Non-emission-line objects

In total, for 49 candidates no (trustworthy) emission lines were detected. We divided them into three categories.

3.3.1. Absorption-line galaxies

For nine non-emission line objects the signal-to-noise ratio of our spectra was sufficient to detect absorption lines, allowing the determination of redshifts. The data are presented in Table 7.

3.3.2. Stellar objects

To separate the stars among the objects with no detectable emission lines, we cross-correlated a list of the most common stellar features with the observed spectra. In total, 26 objects with definite stellar spectra and redshifts close to zero were identified. All of them were crudely classified in categories from definite A-stars to G-stars, with most of them intermediate between A and F. The data for these stars are presented in Table 8.

3.3.3. Non-classified objects

It was not possible to classify 13 objects without emission lines. Their spectra have too low signal-to-noise ratio to detect trustworthy absorption features, or the EWs of their emission lines are too small.

4. Discussion

4.1. The sixth list

As a result we have 182 observed candidates preselected on HQS objective prism plates, out of which 76 were first priority candidates and 106 were second priority. 134 objects (73 % of the total) are found to be either ELGs (126) or quasars (8). 24 of these ELGs were presented in the previous HSS papers, and were reobserved in order to improve the data quality.

Seventy two out of 126 ELGs (~ 57 %) were classified based on the character of their spectra and their luminosity as $HII/BCGs$ or probable BCGs.

14 ELGs are difficult to classify due to their poor signal-to-noise spectra. Six more ELGs were classified as Active Galactic Nuclei (AGN): 4 as Seyfert galaxies and 2 as LINERs. The remaining 33 ELGs are objects with low

excitation: either starburst nuclei galaxies (SBN and probable SBN) or their lower mass analogs – dwarf amorphous nuclear starburst galaxies (DANS or probable DANS).

4.2. Brief summary of the HSS for ELGs

Summarizing the results of the Hamburg/SAO survey presented in Papers I through VI, we discovered altogether, from the 1-st priority candidates, 463 new emission-line objects (26 of them are QSOs). For 100 more ELGs known from the literature (NED) we obtained quantitative data for their emission lines. The total number of confident or probable blue compact/HII-galaxies is 387. Relative to all observed 537 ELGs the fraction of BCGs is $\sim 72\%$.

42 more new BCGs and 56 other ELGs are found among the second priority candidates. Along with the BCGs selected from the HSS candidates, but not observed by us since they already were known from other surveys in this region, the total number of BCGs in the sky region covered by the HSS (~ 1700 sq.degrees of a single piece of sky) reaches ~ 500 . This constitutes the largest and deepest BCG sample in both hemispheres and will be presented elsewhere as a separate publication. The assembly and verifying of the whole HSS database is underway, and the most up-dated version of this will appear at: <http://precise.sao.ru>.

In Figure 1(a-d) we show the distributions of radial velocities, apparent and absolute magnitudes and EWs([O III] 5007) for all found BCGs or BCGs? in the zone of HSS (506 objects, including also the galaxies, selected by us as the HSS candidates, but not observed in this project due to lack of observing time; these objects were already known/classified and had redshift data). The latter group comprises about 70 galaxies which came mainly from the papers by Peimbert & Torres-Peimbert (1992), Vogel et al. (1993), Popescu et al. (1996, 1997, 1998), Ugryumov et al. (1998), Popescu & Hopp (2000) and some unpublished data on BCGs in the SBS zone, partly intersecting the HSS zone.

Since for most of the sample galaxies the total B -band magnitudes are not available, we used their photographic blue magnitudes from the Palomar Sky Survey, as provided in the APM database (Automatic Plate-measuring Machine at Cambridge, Irwin 1998), and calibrated them through the sample of about a hundred BCGs with CCD-measured total B magnitudes. We obtained the linear regression of:

$$B_{\text{CCD}} = 0.429 \times B_{\text{APM}} + 10.51, \quad (1)$$

in the range of B_{APM} from 14 to 19.5, with the standard deviation of residuals of 0.43 mag. These B magnitudes were used as a first approximation to more accurate data in order to estimate absolute magnitudes and to look at the distributions of the sample galaxies of these parameters.

The distributions shown in Figure 1 have the characteristics presented in Table 3. A rough estimate of

Table 3. Characteristics of the HSS BCG sample

Parameter	Number of BCGs	Mean	Median	80% interval
B_{tot} (mag)	506	17.66	17.81	16.51,18.59
M_B (mag)	506	-17.25	-17.40	-15.40,-18.89
V_{hel} (km s^{-1})	506	8471	8752	2695,14976
EW(5007)(\AA)	502	122	113	33,524

the completeness level from the shown distribution is $B_{\text{tot}} = 18.0$. The radial velocity distribution peaks near $V=7500 \text{ km s}^{-1}$, while the distribution of EW(5007) peaks at the value of $\sim 60 \text{ \AA}$.

4.3. Use of the HSS ELG sample

Since the new BCG sample is the largest sample of low-mass galaxies and is well situated on the sky, it can be used for several purposes. First, as it was assumed in planning this survey, such a sample is suitable to address the problem of the spatial distribution of low-mass galaxies relative to the structures delineated by bright galaxies. A more detailed study of the already-known differences between luminous and faint galaxies (e.g., Salzer 1989; Pustilnik et al. 1995; Popescu et al. 1997) could help to gain a deeper understanding of the CDM structure N-body simulations (e.g., such as by Mathis & White 2002 and Gottlöber et al. 2003).

One of the aims of the HSS project was to close the gap between the sky regions of the SBS and Case survey. This goal has now been reached. Since the HSS has intersections with both, the possible differences in their selection functions and other sample characteristics can be quantified and accounted for. Thus, the useful ranges of galaxy parameters for which ELGs can be studied in the whole region of sky covered by the SBS, HSS and Case will be obtained.

Another important aspect of the BCG studies is related to the starburst triggering mechanisms. It can be addressed with the HSS sample to check the preliminary conclusion about the important role of galaxy interactions made, e.g., on the large sample of the SBS BCGs (Pustilnik et al. 2001). Similar studies have been conducted on the samples from the 2dF Survey project by Lambas et al. (2003) and Alonso et al. (2004).

One more interesting aspect of statistical studies of this BCG sample is related to the high S/N ratio spectra of the subsample of the most strong-lined ELGs. This allows us to determine in a large sample of galaxies the abundance of oxygen and other heavy elements by the classic T_e method, and to use these data to compare the BCG properties with the models of galaxy chemical evolution. We already obtained such data for a significant fraction of the HSS BCG sample ($\sim 15\%$ of all BCG and $\sim 40\%$ BCGs with the $\text{EW}([\text{O III}]\lambda 5007) > 150 \text{ \AA}$, Pustilnik et al.

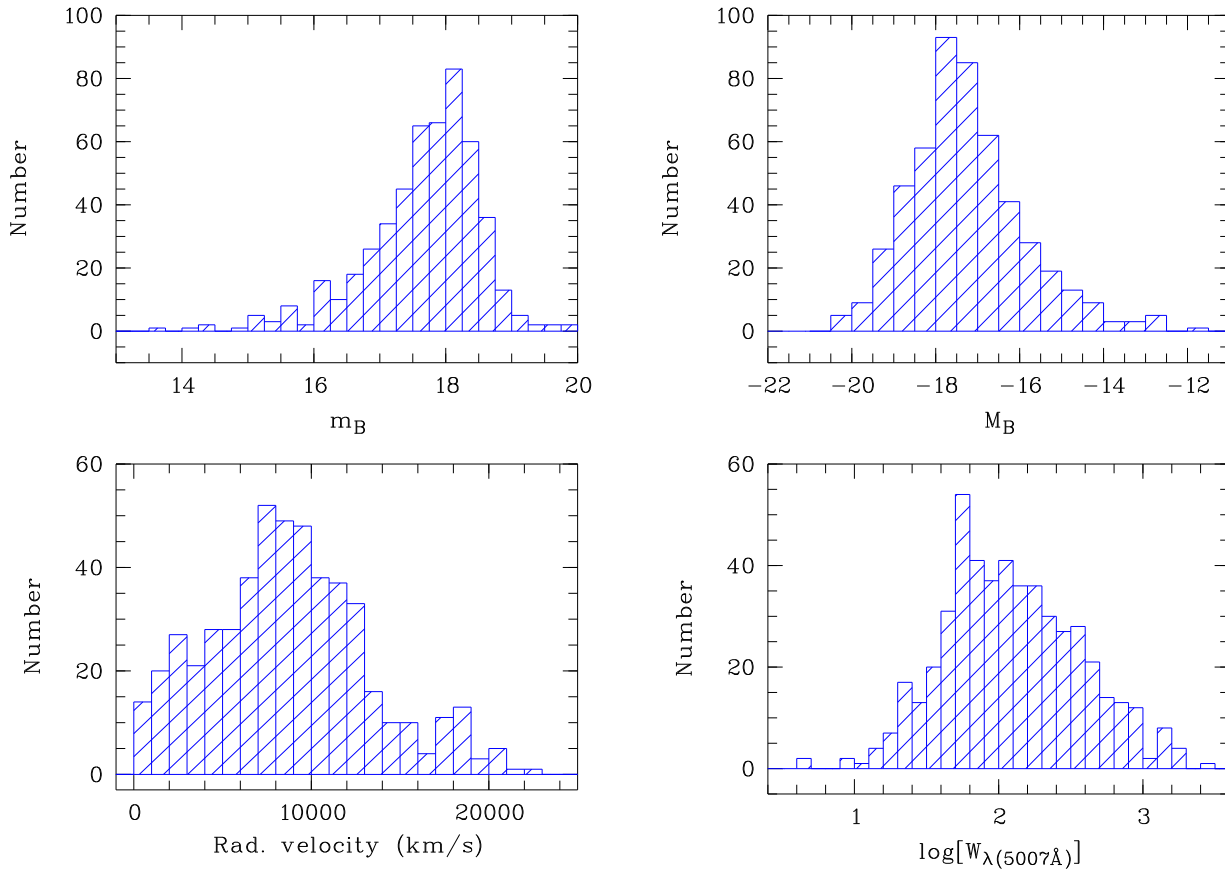


Fig. 1. Distributions of the BCG sample in the zone of HSS of a) total B -magnitude, b) absolute B -magnitude, c) radial velocity and d) equivalent width of $[\text{O III } 5007]$ line.

2004b). Some of the strong-lined HSS BCGs were used in the new primordial helium determination (Izotov & Thuan 2004).

One of the goals of the HSS project was to search for new extremely metal-deficient (XMD) BCGs (those with $12 + \log(\text{O}/\text{H}) \leq 7.65$), possible analogs of candidate young galaxies, like I Zw 18 and SBS 0335-052. Altogether, in addition to the two XMD galaxies in this zone known from previous studies ($1415 + 437 = \text{CG } 389$ and $1224 + 3756 = \text{CG } 1024$), eight new such galaxies are found (see papers by Kniazev et al. 1998, 2000a, 2000b, Pustilnik et al. 2004a, 2004b, Guseva et al. 2003). Thus, the fraction of XMD BCGs at the magnitude limit of the HSS is $\sim 2\%$ (as already claimed by Pustilnik et al. 2003), about ~ 1.5 times higher than the fraction found by Kniazev et al. (2003) for the Sloan Digital Sky Survey (SDSS). While we are dealing with small samples in either case, which makes this ratio uncertain, the ratio still indicates that we succeeded in creating a design for the HSS which is more sensitive in finding XMD BCGs than general galaxy surveys like the SDSS.

5. Conclusions

We performed the follow-up spectroscopy of the sixth and last list of candidates for ELGs (mainly of H II type) from

the Hamburg/SAO Survey. Summarizing the results, the analysis of the spectral information and the discussion above we draw the following conclusions:

- The methods to detect ELG candidates on the plates of the Hamburg Quasar Survey give a reasonably high detection rate of H II type emission-line objects. In total, within the two defined priority categories, 182 objects were observed, 27 of which were already known as ELGs. Among the remaining 155 objects we found 107 emission-line objects corresponding to a detection rate of $\sim 68\%$.
- Besides ELGs we also found 8 new quasars, with either $\text{Ly}\alpha$, or $\text{CIV}\lambda 1549$, or $\text{MgII}\lambda 2798$ in the wavelength region $4950 - 5100 \text{ \AA}$ near the red boundary of the IIIa-J photoplates ($z \sim 3, 1.7$ and 0.8 , respectively).
- The fraction of BCG/H II galaxies among all new observed ELGs (about 43%) is lower in this paper compared to the previous parts of the HSS since about $2/3$ of the observed candidates came from the second priority list.
- This list completes the classification work on the strong-lined ELGs in the zone of the Hamburg/SAO survey. Together with previously-known BCG/H II galaxies in this zone, this sample of ~ 500 objects is the largest one made to date in a well bound region.

Acknowledgements. This work was supported by the grant of the Deutsche Forschungsgemeinschaft No. 436 RUS 17/77/94 and by the Russian Federal Program "Astronomy". U.A.V. is very grateful to the staff of the Hamburg Observatory for their hospitality and kind assistance. Support by the INTAS grant No. 96-0500 is gratefully acknowledged. I.M. and J.M. acknowledge financial support by DGICYT grants AYA2001-2089 and AYA2003-00128 and the Junta de Andalucía. The authors thank the anonymous referee for useful comments and suggestions. The use of APM facility was very important for selection methods for additional candidates to BCGs from the 2nd priority list. This research has made use of the NASA/IPAC Extragalactic Database (NED) which is operated by the Jet Propulsion Laboratory, California Institute of Technology, under contract with the National Aeronautics and Space Administration. We have also used the Digitized Sky Survey, produced at the Space Telescope Science Institute under government grant NAG W-2166.

References

- Afanasiev, V.L., Burenkov, A.N., Vlasyuk, V.V., Drabek, S.V. 1995, SAO RAS internal report, No. 234
- Alonso, M.S., Tissera, P.B., Coldwell, G. & Lambas, D.G. 2004, MNRAS, 352,1081
- Bade, N., Engels, D., Voges, W., et al. 1998, A&AS, 127, 145
- Bohlin, R. C. 1996, AJ, 111, 1743
- Engels, D., Cordis, L., & Köhler, T. 1994, Proc. IAU Symp. 161, ed. H. T. MacGillivray (Kluwer: Dordrecht), 317
- Gottlöber, S., Lokas, E., Klypin, A., Hoffman, Y. 2003, MNRAS, 344, 715
- Grupe, D., Beuermann, K., Thomas, H.-C., Mannheim, K., Fink, H.H. 1998, A&A, 330, 25
- Guseva, N.G., Papaderos, P., Izotov, Y.I., et al. 2003, A&A, 407, 91
- Hagen, H.-J., Groote, D., Engels, D., & Reimers, D. 1995, A&AS, 111, 195
- Hopp, U., Engels, D., Green, R., et al. 2000, A&AS, 142, 417 (**Paper III**)
- Huchra, J.P., Geller, M.J., & Corwin, H.G. Jr. 1995, ApJS, 99, 391
- Irwin, M. 1998, <http://www.ast.cam.ac.uk/~apmcat/>
- Izotov, Y.I., & Thuan, T.X. 2004, ApJ, 602, 200
- Kniazev, A.Y., & Shergin, V.S. 1995, SAO RAS internal report, 249, 1
- Kniazev, A.Y., Pustilnik, S.A., Ugryumov, A.V. 1998, Bulletin SAO, 46, 23
- Kniazev, A.Y., Pustilnik, S.A., Ugryumov, A.V., & Kniazeva, T.F. 2000a, Astronomy Letters, 26, 129
- Kniazev, A.Y., Pustilnik, S.A., Masegosa, J., et al. 2000b, A&A, 357, 101
- Kniazev, A.Y., Engels, D., Pustilnik, S.A. et al. 2001, A&A, 366, 771 (**Paper IV**)
- Kniazev, A.Y., Grebel, E.K., Lei Hao, et al. 2003, ApJ, 593, L73
- Kniazev, A.Y., Pustilnik, S.A., Grebel, E.K., Lee, H., & Pramskij, A.G. 2004, ApJS, 153, 429
- Lambas, D.G., Tissera, P. B., Alonso, M. S., & Coldwell, G. 2003, MNRAS, 346, 1189
- Markarian, B.E., Lipovetsky, V.A., & Stepanian, J.A. 1983, Afz, 19, 29
- Mathis, H. & White, S.D.M. 2002, MNRAS, 337, 1193
- Oke, J.B. 1990, AJ, 99, 1621
- Peimbert, M., & Torres-Peimbert, S. 1992, A&A, 253, 349
- Pesch, P., Stephenson, C.B., & MacConnell, D.J. 1995, ApJS, 98, 41
- Popescu, C. C., & Hopp, U. 2000, A&AS, 142, 247
- Popescu, C.C., Hopp, U., Hagen, H.-J., & Elsässer, H. 1996, A&AS, 116, 43
- Popescu, C.C., Hopp, U., & Elsässer, H. 1997, A&A, 325, 881
- Popescu, C.C., Hopp, U., Hagen, H.-J., Elsässer, H. 1998, A&AS, 133, 13
- Pustilnik, S.A., Ugryumov, A.V., Lipovetsky, V.A., Thuan, T.X., & Guseva, N.G. 1995, ApJ, 443, 499
- Pustilnik, S.A., Engels, D., Ugryumov, A.V., et al. 1999, A&AS, 135, 299 (**Paper II**)
- Pustilnik, S.A., Kniazev, A.Y., Lipovetsky, V.A., & Ugryumov, A.V. 2001, A&A, 373, 24
- Pustilnik, S.A., Kniazev, A.Y., Pramskij, A.G., & Ugryumov, A.V. 2003, Proc. of Euroconference "The evolution of galaxies. III. From simple approaches to self-consistent models", Kiel, Germany, July 2002, ApSS, 284, 795
- Pustilnik, S.A., Kniazev, A.Y., Pramskij, A.G. et al. 2004a, A&A, 419, 469
- Pustilnik, S.A., Kniazev, A.Y., Pramskij, A.G., et al. 2004b, A&A, in preparation
- Salzer, J.J. 1989, ApJ, 347, 152
- Salzer, J.J., MacAlpine, G.M., & Boroson, T.A. 1989, ApJS, 70, 479
- Salzer, J.J., Moody, J.W., Rosenberg, J.L., Gregory, S.A., & Newberry, M.V. 1995, AJ, 109, 2376
- Salzer, J.J., Gronwall, C., Lipovetsky, V.A., et al. 2000, AJ, 120, 80
- Schneider, D.P., Schmidt, M., Gunn, J.E. 1994, AJ, 107, 1245
- Stepanian, J.A. 1994, Proc. IAU Symp. 161, ed. H. T. MacGillivray (Kluwer: Dordrecht), 731
- Ugryumov, A.V., Pustilnik, S.A., Lipovetsky, V.A., Izotov, Y.I., & Richter, G.M. 1998, A&AS, 131, 295
- Ugryumov, A.V., Engels, D., Lipovetsky, V.A., et al. 1999, A&AS, 135, 511 (**Paper I**)
- Ugryumov, A.V., Engels, D., Kniazev, A.Y. et al. 2001, 2001, A&A, 374, 907 (**Paper V**)
- Vogel, S., Engels, D., Hagen, H.-J., et al. 1993, A&AS, 98, 193

Table 4. Coordinates, velocities and magnitudes of emission-line galaxies

#	Name	α (1950)	δ (1950)	$V_{hel}^a \pm \sigma_V$	m_B	M_B^b	Type	Other names from NED and number of reference
	(2)	(3)	(4)	(5)	(6)	(7)	(8)	(9)
1	HS 0713+4105 [‡]	07 13 28.5	+41 05 51	13768 \pm 40	*17.00	-19.31	BCG	2MASX J07165730+4100327
2	HS 0719+4928 [‡]	07 19 00.7	+49 28 19	18659 \pm 40	17.60	-19.37	SBN?	
3	HS 0727+4711 [‡]	07 27 52.1	+47 11 51	20192 \pm 30	18.00	-19.15	SBN?	2MASX J07313250+4705296
4	HS 0732+3529	07 32 23.3	+35 29 07	3785 \pm 42	17.80	-15.71	BCG?	(1)
5	HS 0735+4507 [‡]	07 35 50.8	+45 07 47	15259 \pm 50	18.50	-18.04	NON	
6	HS 0755+4142 [‡]	07 55 42.3	+41 42 43	26702 \pm 54	18.00	-19.75	SBN	2MASX J07590777+4134301
7	HS 0756+4402 [‡]	07 56 51.8	+44 02 21	16189 \pm 30	17.90	-18.77	SBN?	
8	HS 0807+4103 [‡]	08 07 58.7	+41 03 48	20073 \pm 110	*17.57	-19.56	Sy1	FIRST J081121.4+40545
9	HS 0817+4600	08 17 35.5	+46 00 26	11319 \pm 48	17.40	-18.49	BCG	2MASX J08210576+4550542 (2)
10	HS 0820+3919 [‡]	08 20 32.1	+39 19 23	6963 \pm 35	18.50	-16.33	BCG	
11	HS 0849+3639 [‡]	08 49 34.0	+36 39 14	7467 \pm 42	20.00	-14.99	BCG	(3)
12	HS 0859+4738 [‡]	08 59 14.6	+47 38 01	15760 \pm 40	18.80	-17.81	NON	
13	HS 0903+4349	09 03 31.9	+43 49 45	7758 \pm 40	20.20	-14.87	BCG	(1)
14	HS 0907+4444	09 07 59.1	+44 44 42	8003 \pm 42	18.40	-16.74	BCG	
15	HS 0919+4234	09 19 07.8	+42 34 15	9856 \pm 38	18.70	-16.89	BCG	
16	HS 0925+4821 [‡]	09 25 25.4	+48 21 35	23557 \pm 40	17.80	-19.68	SBN	
17	HS 0932+3616 [‡]	09 32 22.6	+36 16 57	8005 \pm 38	18.10	-17.04	SBN	
18	HS 0935+4931	09 35 04.5	+49 31 49	9334 \pm 40	17.90	-17.57	BCG	SBS 0935+495 (2)
19	HS 0944+3633 [‡]	09 44 56.0	+36 33 45	7876 \pm 40	18.00	-17.10	BCG	
20	HS 0947+3537 [‡]	09 47 47.0	+35 37 09	12110 \pm 50	17.50	-18.54	SBN	
21	HS 0948+3723	09 48 19.0	+37 23 05	4784 \pm 40	*18.14	-15.88	BCG	(3,4)
22	HS 0951+3841	09 51 46.4	+38 41 13	5233 \pm 30	16.80	-17.41	BCG	(1)
23	HS 1009+4906 [‡]	10 09 58.3	+49 06 28	18321 \pm 40	*17.89	-19.05	BCG	2MASX J10130712+4851368
24	HS 1010+4907	10 10 00.3	+49 07 09	18246 \pm 40	*18.23	-18.70	BCG	
25	HS 1012+4135	10 12 41.1	+41 35 48	20485 \pm 30	18.00	-19.18	BCG	
26	HS 1014+3923 [‡]	10 14 45.9	+39 23 20	15596 \pm 30	18.00	-18.59	BCG	
27	HS 1024+4041	10 24 49.3	+40 41 39	13239 \pm 63	17.70	-18.53	SBN?	MAPS-NGP O_214_1065413
28	HS 1027+4018	10 27 01.3	+40 18 48	28310 \pm 51	*18.21	-19.67	LINER	2MASX J10295708+4003288
29	HS 1034+3722 [‡]	10 34 49.2	+37 22 33	8584 \pm 38	17.30	-17.99	BCG	
30	HS 1037+4757	10 37 30.5	+47 57 38	10130 \pm 80	18.50	-17.15	BCG	(2)
31	HS 1043+3851 [‡]	10 43 17.6	+38 51 51	7991 \pm 61	19.60	-15.53	BCG	
32	HS 1043+4711	10 43 56.1	+47 11 32	10027 \pm 40	*16.89	-18.74	SBN?	KUG 1043+471
33	HS 1052+4458	10 52 53.4	+44 58 53	15384 \pm 30	*18.25	-18.31	BCG	MAPS-NGP O_169_1616461
34	HS 1053+3624 [‡]	10 53 52.9	+36 24 30	816 \pm 40	17.90	-12.28	NON	MAPS-NGP O_264_0140714
35	HS 1054+4605	10 54 34.0	+46 05 13	6864 \pm 30	16.60	-18.20	BCG	(5)
36	HS 1057+4317	10 57 34.8	+43 17 16	11155 \pm 45	*16.80	-19.06	BCG	2MASX J11002494+4301119
37	HS 1102+5009	11 02 45.3	+50 09 53	8465 \pm 70	18.10	-17.18	BCG	(2)
38	HS 1113+4622	11 13 02.9	+46 22 58	2925 \pm 38	17.90	-15.05	BCG	(5)
39	HS 1117+4722	11 17 36.5	+47 22 23	7467 \pm 40	17.10	-17.89	SBN	2MASX J11202304+4705592 (2)
40	HS 1120+4453 [‡]	11 20 31.5	+44 53 12	9722 \pm 40	*17.68	-17.88	NON	MAPS-NGP O_170_0535959

Table 4. (Continued)

#	Name	α (1950)	δ (1950)	$V_{hel}^a \pm \sigma_V$	m_B	M_B^b	Type	Other names from NED and number of reference
	(2)	(3)	(4)	(5)	(6)	(7)	(8)	(9)
41	HS 1121+4707	11 21 02.4	+47 07 25	10490 \pm 38	19.30	-16.42	BCG	
42	HS 1122+4230	11 22 10.3	+42 30 56	13371 \pm 30	*16.87	-19.38	SBN	KUG 1122+425, CG1424
43	HS 1123+4716	11 23 01.9	+47 16 29	10115 \pm 46	16.50	-19.15	BCG	MRK 0168 (2)
44	HS 1128+4753	11 28 27.0	+47 53 29	13230 \pm 63	19.00	-17.23	BCG	PC 1128+4753 (6)
45	HS 1134+3639	11 34 15.7	+36 39 52	1525 \pm 40	17.10	-14.50	BCG	(1)
46	HS 1143+3630 [‡]	11 43 18.6	+36 30 47	11345 \pm 40	*17.85	-18.04	NON	2MASX J11455560+3614074
47	HS 1145+4746	11 45 30.9	+47 46 09	30267 \pm 42	18.20	-19.83	NON	
48	HS 1148+4704 [‡]	11 48 12.5	+47 04 58	12673 \pm 100	18.00	-18.19	SBN	
49	HS 1150+4841 [‡]	11 50 14.9	+48 41 58	4345 \pm 40	19.40	-14.41	BCG	
50	HS 1151+4917 [‡]	11 51 15.8	+49 17 30	16493 \pm 58	18.10	-18.61	SBN	MAPS-NGP O_171_0059619
51	HS 1156+4151	11 56 10.3	+41 51 06	38017 \pm 40	*18.39	-20.13	SBN	FBQS J115844.6+413426
52	HS 1200+3720 [‡]	12 00 56.9	+37 20 42	12908 \pm 40	*18.29	-17.88	NON	MAPS-NGP O_267_0076646
53	HS 1204+3755 [‡]	12 04 46.3	+37 55 29	22062 \pm 40	*18.52	-18.82	NON	MAPS-NGP O_267_0042638
54	HS 1205+3920 [‡]	12 05 15.0	+39 20 37	11140 \pm 40	*16.54	-19.31	SBN?	CG 1515
55	HS 1208+4902	12 08 02.5	+49 02 29	12085 \pm 60	20.30	-15.74	BCG	(2)
56	HS 1215+3820 [‡]	12 15 20.7	+38 20 19	15149 \pm 40	*17.87	-18.65	NON	MAPS-NGP O_267_0031716
57	HS 1216+4148 [‡]	12 16 50.3	+41 48 54	7210 \pm 40	*17.83	-17.08	BCG	
58	HS 1224+4834 [‡]	12 24 37.6	+48 34 31	7872 \pm 40	19.40	-15.70	DANS	MAPS-NGP O_172_0100617
59	HS 1224+5022 [‡]	12 24 51.9	+50 22 15	7122 \pm 40	19.80	-15.08	BCG	
60	HS 1225+4817 [‡]	12 25 04.0	+48 17 58	13631 \pm 79	18.30	-17.99	NON	MAPS-NGP O_172_0110882
61	HS 1231+4349 [‡]	12 31 36.8	+43 49 48	44427 \pm 73	*17.87	-20.99	SBN	
62	HS 1235+4108 [‡]	12 35 35.1	+41 08 37	32516 \pm 50	*17.74	-20.44	SBN	
63	HS 1239+4022	12 39 16.4	+40 22 00	7186 \pm 40	19.70	-15.20	BCG	
64	HS 1240+4423	12 40 09.2	+44 23 35	12361 \pm 40	18.80	-17.28	BCG	
65	HS 1241+4418 [‡]	12 41 39.8	+44 18 37	12518 \pm 32	*17.64	-18.47	SBN?	MAPS-NGP O_218_0037592
66	HS 1243+4304	12 43 19.5	+43 04 20	11688 \pm 30	18.40	-17.56	BCG	
67	HS 1247+3929 [‡]	12 47 16.1	+39 29 55	12186 \pm 40	*18.16	-17.89	BCG	
68	HS 1253+3853 [‡]	12 53 23.4	+38 53 42	9418 \pm 40	17.30	-18.19	SBN	
69	HS 1254+4708	12 54 53.6	+47 08 59	10103 \pm 32	18.40	-17.24	BCG	(5)
70	HS 1256+3512	12 56 51.2	+35 12 19	907 \pm 43	16.80	-13.61	DANS?	2MASX J12591328+3456110 (7)
71	HS 1256+4046	12 56 56.1	+40 46 49	5842 \pm 40	*18.67	-15.78	BCG	
72	HS 1258+4510	12 58 41.0	+45 10 05	11690 \pm 40	*17.83	-18.13	SBN	
73	HS 1259+3848 [‡]	12 59 36.6	+38 48 17	15621 \pm 40	17.00	-19.59	SBN	2MASX J13015634+3832108
74	HS 1305+4511	13 05 47.6	+45 11 46	10215 \pm 40	*18.02	-17.65	BCG	
75	HS 1310+3801	13 10 32.3	+38 01 04	6447 \pm 64	*18.47	-16.21	BCG?	PC 1310+3801 (6,8)
76	HS 1311+3944 [‡]	13 11 17.2	+39 44 04	13317 \pm 63	17.30	-18.94	BCG	MAPS-NGP O_219_0887656
77	HS 1320+4415	13 20 56.8	+44 15 44	8213 \pm 40	*18.20	-16.99	BCG	
78	HS 1325+4823	13 25 45.5	+48 23 35	18278 \pm 40	18.30	-18.63	BCG	
79	HS 1330+4351	13 30 14.6	+43 51 00	36866 \pm 40	*17.87	-20.58	LINER	2MASX J13322375+4335356
80	HS 1331+3708 [‡]	13 31 41.8	+37 08 39	7475 \pm 40	18.70	-16.29	SBN?	

Table 4. (Continued)

#	Name	α (1950)	δ (1950)	$V_{hel}^a \pm \sigma_V$	m_B	M_B^b	Type	Other names from NED and number of reference
	(2)	(3)	(4)	(5)	(6)	(7)	(8)	(9)
81	HS 1333+3522 [‡]	13 33 30.5	+35 22 58	6691 \pm 40	17.40	-17.35	BCG	MAPS-NGP O_270_0867227
82	HS 1340+3806 [‡]	13 40 18.2	+38 06 02	6676 \pm 40	18.70	-16.04	BCG	NGP9 F270-0161337
83	HS 1340+4428	13 40 45.3	+44 28 47	13233 \pm 42	*17.60	-18.63	BCG	MAPS-NGP O_220_0009424
84	HS 1341+4318	13 41 53.4	+43 18 22	8030 \pm 40	*18.43	-16.71	BCG	MAPS-NGP O_220_0094354
85	HS 1353+4706B	13 53 25.7	+47 06 30	8347 \pm 40	18.70	-16.53	BCG	
86	HS 1356+4159	13 56 45.8	+41 59 34	13011 \pm 60	17.90	-18.29	BCG	(2)
87	HS 1358+4447	13 58 36.4	+44 47 08	12203 \pm 53	17.00	-19.05	BCG	MAPS-NGP O_175_2534150
88	HS 1407+3540 [‡]	14 07 23.0	+35 40 35	3375 \pm 50	16.80	-16.46	BCG	MAPS-NGP O_271_0157627
89	HS 1417+4011 [‡]	14 17 12.1	+40 11 15	7735 \pm 40	17.60	-17.46	BCG	MAPS-NGP O_221_0343989
90	HS 1417+4027	14 17 36.1	+40 27 32	12784 \pm 55	*17.78	-18.37	BCG	MAPS-NGP O_221_0327684
91	HS 1423+4712 [‡]	14 23 12.1	+47 12 37	10056 \pm 40	18.80	-16.83	BCG	MAPS-NGP O_175_1814530
92	HS 1424+3558 [‡]	14 24 01.0	+35 58 21	8555 \pm 48	*17.29	-17.99	DANS?	MAPS-NGP O_272_0768607
93	HS 1426+3658 [‡]	14 26 16.4	+36 58 15	30091 \pm 93	*18.32	-19.69	NON	
94	HS 1437+3724 [‡]	14 37 51.9	+37 24 57	29990 \pm 40	*18.00	-20.01	NON	MAPS-NGP O_272_0419870
95	HS 1439+3704 [‡]	14 39 08.9	+37 04 46	33365 \pm 40	*18.25	-19.99	NON	
96	HS 1510+5019	15 10 15.8	+50 19 37	9849 \pm 34	17.20	-18.39	BCG	SBS 1510+503, CG657 (2)
97	HS 1525+4344 [‡]	15 25 48.2	+43 44 22	46466 \pm 122	*18.15	-20.81	Sy1	
98	HS 1536+4557	15 36 44.2	+45 57 49	6579 \pm 65	17.20	-17.51	BCG	(5)
99	HS 1543+3602	15 43 12.5	+36 02 46	1997 \pm 54	16.00	-16.12	BCG	(1)
100	HS 1545+4641	15 45 21.7	+46 41 22	8894 \pm 50	18.60	-16.77	BCG	
101	HS 1547+4421	15 47 53.3	+44 21 00	5834 \pm 40	18.00	-16.45	BCG	
102	HS 1605+4440 [‡]	16 05 40.9	+44 40 58	12570 \pm 40	17.70	-18.42	SBN	
103	HS 1607+3621 [‡]	16 07 54.2	+36 21 09	9201 \pm 48	17.20	-18.24	SBN?	2MASX J16094449+3613227
104	HS 1613+3902	16 13 51.4	+39 02 28	10036 \pm 40	18.70	-16.93	BCG	(3)
105	HS 1614+4450 [‡]	16 14 04.3	+44 50 01	24637 \pm 40	17.90	-19.68	SBN?	
106	HS 1616+4023 [‡]	16 16 18.1	+40 23 47	8739 \pm 54	17.50	-17.83	BCG	
107	HS 1624+4143 [‡]	16 24 27.0	+41 43 25	8278 \pm 56	17.90	-17.31	BCG?	
108	HS 1627+3625 [‡]	16 27 15.0	+36 25 54	22664 \pm 40	18.20	-19.20	Sy1	RX J1629.0+3619
109	HS 1629+4513	16 29 34.2	+45 13 44	17267 \pm 40	18.40	-18.41	BCG	(5)
110	HS 1629+4820	16 29 27.8	+48 20 16	2710 \pm 40	18.60	-14.19	BCG	
111	HS 1636+4319	16 36 56.5	+43 19 22	9499 \pm 43	17.50	-18.01	BCG	
112	HS 1637+4206	16 37 13.3	+42 06 29	9717 \pm 40	18.80	-16.76	NON	
113	HS 1644+3934 [‡]	16 44 44.6	+39 34 50	30149 \pm 65	*17.30	-20.72	Sy2	RX J1646+3929 (9,10)
114	HS 1645+3551	16 45 51.9	+35 51 57	6760 \pm 40	17.70	-17.07	BCG	(4)
115	HS 1645+4211	16 45 21.2	+42 11 29	8525 \pm 47	18.10	-17.17	BCG	
116	HS 1645+4401 [‡]	16 45 39.1	+44 01 42	7957 \pm 40	*17.17	-17.95	SBN	
117	HS 1651+4933	16 51 16.6	+49 33 46	8806 \pm 51	18.00	-17.34	BCG	
118	HS 1700+4907	17 00 00.0	+49 07 20	9353 \pm 32	16.90	-18.58	BCG	2MASX J17011928+4903063
119	HS 1702+4146 [‡]	17 02 31.2	+41 46 15	4888 \pm 61	*17.94	-16.13	BCG	
120	HS 1711+3756	17 11 41.5	+37 56 12	8304 \pm 60	17.60	-17.62	BCG	(4)

Table 4. (Continued)

#	Name	α (1950)	δ (1950)	$V_{hel}^a \pm \sigma_V$	m_B	M_B^b	Type	Other names from NED and number of reference
	(2)	(3)	(4)	(5)	(6)	(7)	(8)	(9)
121	HS 1715+4827	17 15 10.3	+48 27 25	8735 ± 62	19.80	-15.53	BCG	
122	HS 1720+4720	17 20 55.3	+47 20 50	7964 ± 45	17.80	-17.33	SBN	
123	HS 1723+4410	17 23 40.2	+44 10 07	15789 ± 40	*17.55	-19.06	SBN?	2MASX J17250981+4407314
124	HS 1724+4001	17 24 29.7	+40 01 59	10367 ± 40	*18.25	-17.45	SBN	
125	HS 1730+4601	17 30 55.3	+46 01 17	11049 ± 45	18.40	-17.44	BCG	
126	HS 1733+4035	17 33 57.1	+40 35 30	9848 ± 54	*17.63	-17.96	SBN	

^a Heliocentric velocities.; ^b absolute magnitudes are not corrected for galactic extinction;

* means APM magnitudes; † galaxies from the APM selected sample (2-nd priority). **1** – Paper IV (Kniazev et al. 2001);

2 – Paper II (Pustilnik et al. 1999); **3** – Paper V (Ugryumov et al. 2001); **4** – Paper III (Hopp et al. 2000);

5 – Paper I (Ugryumov et al. 1999); **6** – Schneider et al. (1994); **7** – Popescu et al. (1996); **8** – Popescu et al. (1998)

9 – Grupe et al. (1998); **10** - Bade et al. (1998)

Table 5. Emission line parameters

#	Name	T	F(H β)	$\frac{F(3727)}{F(H\beta)}$	$\frac{F(5007)}{F(H\beta)}$	$\frac{F(H\alpha)}{F(H\beta)}$	$\frac{F(6583)}{F(H\alpha)}$	$\frac{F([SII])}{F(H\alpha)}$	EW ₃₇₂₇	EW _{Hβ}	EW ₅₀₀₇
	(2)	(3)	(4)	(5)	(6)	(7)	(8)	(9)	(10)	(11)	(12)
1	HS 0713+4105*	C	41 ^b	1.84 ^d	3.15 ^b	4.90 ^b	0.15 ^b	0.23 ^b	33 ^c	26 ^b	82 ^a
2	HS 0719+4928*†	B	14 ^b	2.92 ^c	1.77 ^c	5.45 ^b	0.25 ^b	0.29 ^b	27 ^b	8 ^b	13 ^b
3	HS 0727+4711*	B	20 ^c	2.86 ^c	1.12 ^c	5.53 ^c	0.37 ^b	0.29 ^b	46 ^c	11 ^c	12 ^c
4	HS 0732+3529	B	44 ^b	1.27 ^c	6.17 ^c				53 ^c	55 ^b	331 ^a
5	HS 0735+4507 [‡] *	B	10 ^c				0.28 ^d	0.87 ^d			
6	HS 0755+4142 [‡] *	B	34 ^b				0.25 ^d	0.40 ^d	25 ^d		15 ^c
7	HS 0756+4402*†	B	13 ^b	3.60 ^c	3.19 ^c	3.42 ^c	0.16 ^d		130 ^b	14 ^b	33 ^c
8	HS 0807+4103 [‡] *	B	54 ^b				0.38 ^d	0.26 ^d			37 ^b
9	HS 0817+4600*†	B	18 ^a	2.80 ^a	1.76 ^a				39 ^a	10 ^a	16 ^a
10	HS 0820+3919†	B	10 ^b	2.10 ^c	3.16 ^c				48 ^b	16 ^b	51 ^a
11	HS 0849+3639*	B	28 ^b	2.51 ^b	2.54 ^b				159 ^b	71 ^b	184 ^b
12	HS 0859+4738 [‡] *	B	22 ^c				<0.46	<0.55			27 ^d
13	HS 0903+4349*	C	6.1 ^c		7.87 ^c	4.92 ^c	<0.05	0.12 ^d		20 ^c	209 ^a
14	HS 0907+4444*	C	16 ^b		4.05 ^b	4.16 ^b	0.05 ^d	0.15 ^c		23 ^b	96 ^a
15	HS 0919+4234*	C	22 ^b		5.46 ^c	3.02 ^c	<0.09	0.10 ^d		73 ^b	292 ^a
16	HS 0925+4821*	B	7.1 ^d	1.89 ^d	1.19 ^d	4.74 ^d	0.38 ^c	0.39 ^d	34 ^d	8 ^d	10 ^d
17	HS 0932+3616†	B	2.5 ^d	4.34 ^d	2.32 ^d				107 ^d	6 ^d	15 ^c
18	HS 0935+4931†	B	15 ^b	3.71 ^b	3.69 ^b	3.48 ^b	0.09 ^c	0.28 ^b	115 ^a	22 ^b	80 ^a
19	HS 0944+3633†	B	14 ^b	2.61 ^b	2.74 ^b				45 ^b	15 ^b	36 ^a
20	HS 0947+3537	B	8.0 ^a	4.26 ^b	1.14 ^b				40 ^b	8 ^b	10 ^b
21	HS 0948+3723*†	B	3.9 ^b	2.77 ^c	4.31 ^c				39 ^c	7 ^b	32 ^b
22	HS 0951+3841†	B	47 ^a	3.39 ^a	3.17 ^a				82 ^a	24 ^a	72 ^a
23	HS 1009+4906†	B	1.5 ^d	6.57 ^d	5.35 ^d	16.55 ^d	20.10	0.47 ^d	31 ^b	4 ^d	22 ^b
24	HS 1010+4907	B	27 ^a	1.42 ^a	5.59 ^a	14.02 ^d	<0.06	0.07 ^b	134 ^a	257 ^a	1779 ^a
25	HS 1012+4135*	B	29 ^a	2.64 ^a	5.60 ^a	14.27 ^d	0.05	0.10 ^c	87 ^a	47 ^a	268 ^a
26	HS 1014+3923*†	B	18 ^b	3.53 ^b	3.29 ^b				66 ^a	19 ^b	58 ^a
27	HS 1024+4041*	B	3.5 ^d	2.94 ^d	1.30 ^d	5.93 ^d	<0.16	0.33 ^d	25 ^d	9 ^d	12 ^d
28	HS 1027+4018 [‡]	M	33 ^d				2.00 ^c	1.02 ^c	54 ^c		
29	HS 1034+3722†	B	31 ^a	2.15 ^b	4.52 ^a				92 ^a	33 ^a	152 ^a
30	HS 1037+4757	B	1.5 ^c	1.04 ^d	6.42 ^c	5.37 ^c	0.04 ^d	0.33 ^d		17 ^c	176 ^b
31	HS 1043+3851†	C	19 ^a		3.36 ^b	3.07 ^b	0.08 ^d	0.09 ^d		15 ^a	55 ^a
32	HS 1043+4711	C	76 ^a	2.09 ^c	1.47 ^b	3.48 ^a	0.31 ^a	0.24 ^a	66 ^c	31 ^a	49 ^a
33	HS 1052+4458	M	11 ^c	2.94 ^c	4.00 ^c	3.15 ^c	<0.19	<0.18	93 ^c	23 ^c	90 ^a
34	HS 1053+3624*	C	31 ^d		1.00 ^d	6.90 ^d	<0.10			13 ^d	14 ^d
35	HS 1054+4605†	B	31 ^a	3.53 ^a	2.66 ^a				91 ^a	19 ^a	47 ^a
36	HS 1057+4317	M	199 ^a	2.48 ^a	5.06 ^a	3.49 ^a	0.07 ^d	0.16 ^b	97 ^a	43 ^a	223 ^a
37	HS 1102+5009†	M	12 ^c	6.82 ^c	4.31 ^c	6.12 ^c	0.13 ^d	0.30 ^d	100 ^b	8 ^c	33 ^a
38	HS 1113+4622*†	B	25 ^a	2.09 ^a	3.30 ^a				52 ^a	21 ^a	63 ^a
39	HS 1117+4722†	M	100 ^a	2.61 ^b	1.34 ^a	4.29 ^a	0.19 ^b	0.21 ^b	54 ^b	20 ^a	28 ^a
40	HS 1120+4453 [‡]	C	126 ^b				<0.21	<0.16			14 ^c

Table 5. (Continued)

#	Name	T	F(H β)	$\frac{F(3727)}{F(H\beta)}$	$\frac{F(5007)}{F(H\beta)}$	$\frac{F(H\alpha)}{F(H\beta)}$	$\frac{F(6583)}{F(H\alpha)}$	$\frac{F([SII])}{F(H\alpha)}$	EW ₃₇₂₇	EW _{Hβ}	EW ₅₀₀₇
	(2)	(3)	(4)	(5)	(6)	(7)	(8)	(9)	(10)	(11)	(12)
41	HS 1121+4707	M	27 ^b		3.76 ^b	3.36 ^b	<0.09	0.17 ^d		41 ^b	163 ^a
42	HS 1122+4230	M	27 ^c	2.48 ^c	1.04 ^c	6.87 ^c	0.32 ^b	0.36 ^c	26 ^c	9 ^c	9 ^c
43	HS 1123+4716†	B	152 ^a	1.49 ^a	3.48 ^a				97 ^a	50 ^a	160 ^a
44	HS 1128+4753†	C	12 ^b		4.88 ^b	3.07 ^b	<0.11	0.13 ^c		15 ^b	82 ^a
45	HS 1134+3639*†	B	34 ^a		3.78 ^a				98 ^d	18 ^a	66 ^a
46	HS 1143+3630 [‡] *	B	100 ^a				0.35 ^c	0.39 ^d			8 ^d
47	HS 1145+4746 [‡]	M	17 ^c				<0.43				
48	HS 1148+4704*†	B	4.5 ^d			1.89 ^d	0.22 ^d	0.37 ^d		12 ^c	
49	HS 1150+4841*	B	18 ^a	1.03 ^b	3.32 ^b	3.245 ^d	<0.04	<0.05	89 ^c	121 ^a	404 ^b
50	HS 1151+4917*†	B	4.3 ^d	5.39 ^d	1.22 ^d	3.04 ^d	0.24 ^d	0.21 ^d	32 ^d	5 ^d	6 ^c
51	HS 1156+4151†	M	13 ^c	3.07 ^d	3.37 ^c	6.05 ^c	0.21 ^d		42 ^c	8 ^c	24 ^b
52	HS 1200+3720 [‡] *	B	55 ^c								
53	HS 1204+3755 [‡]	C	0.9 ^c								
54	HS 1205+3920*†	B	49 ^b	3.66 ^c	1.68 ^b	5.26 ^b	0.29 ^b	0.39 ^b	59 ^c	8 ^b	15 ^b
55	HS 1208+4902*	B	20 ^a	2.23 ^a	6.71 ^a	1.497 ^d	<0.06	0.10 ^c	95 ^a	47 ^a	274 ^a
56	HS 1215+3820 [‡] *	B	55 ^c								
57	HS 1216+4148†	C	30 ^b		4.22 ^b	2.96 ^b	0.07 ^d	0.18 ^d		17 ^b	70 ^a
58	HS 1224+4834*†	B	4.8 ^c	5.00 ^c	1.76 ^c	3.11 ^c	0.15 ^d	0.45 ^d	72 ^c	10 ^c	16 ^c
59	HS 1224+5022*†	B	8.0 ^c	4.27 ^c	3.50 ^c	2.03 ^d	0.12 ^d	0.23 ^d	153 ^b	44 ^c	108 ^a
60	HS 1225+4817 [‡]	C	53 ^a				0.04 ^d	0.36 ^b			14 ^a
61	HS 1231+4349†	C	44 ^a	2.18 ^a	1.39 ^a	3.53 ^a	0.25 ^c	0.25 ^b	53 ^a	23 ^a	32 ^a
62	HS 1235+4108 [‡] *	C	25 ^a				0.27 ^c	0.36 ^d			4 ^d
63	HS 1239+4022*	C	6.4 ^c		5.54 ^c	2.90 ^c	<0.16	0.32 ^d		12 ^c	78 ^a
64	HS 1240+4423†	C	17 ^b		3.70 ^b	3.52 ^b	0.10 ^c	0.18 ^c		17 ^b	66 ^a
65	HS 1241+4418*	C	2.6 ^d		1.76 ^d	9.68 ^d	0.26 ^d	0.43 ^d		3 ^d	5 ^d
66	HS 1243+4304*†	B	9.6 ^c	3.33 ^c	3.98 ^c	3.80 ^d	<0.10	0.17 ^d	68 ^c	19 ^c	80 ^b
67	HS 1247+3929*	B	23 ^c	2.98 ^c	3.50 ^c	2.94 ^c	0.11 ^d	0.19 ^d	220 ^b	27 ^c	102 ^b
68	HS 1253+3853 [‡]	C	41 ^a				0.26 ^b	0.44 ^c			6 ^b
69	HS 1254+4708*†	B	33 ^a	3.74 ^a	3.40 ^a	1.696 ^a	0.10 ^b	0.25 ^b	92 ^a	20 ^a	62 ^a
70	HS 1256+3512*	B	38 ^d	1.91 ^d	1.54 ^d	2.72 ^d	0.13 ^d	0.17 ^d	50 ^c	34 ^d	49 ^c
71	HS 1256+4046	C	11 ^b		6.26 ^b	4.56 ^b				23 ^b	140 ^a
72	HS 1258+4510†	M	10 ^c	4.98 ^d	0.94 ^d	7.49 ^c	0.39 ^c	0.44 ^c	46 ^c	4 ^c	4 ^d
73	HS 1259+3848†	C	12 ^b		1.68 ^b	4.84 ^b	0.21 ^c	0.42 ^b		8 ^b	13 ^a
74	HS 1305+4511*†	C	35 ^a	1.90 ^c	3.39 ^a	3.252 ^d	0.07 ^c	0.14 ^c	59 ^c	26 ^a	88 ^a
75	HS 1310+3801 [‡] *	B	18 ^d								101 ^c
76	HS 1311+3944*	B	15 ^c	6.10 ^c	4.95 ^c	5.10 ^c	<0.16	0.37 ^d	90 ^b	11 ^c	56 ^b
77	HS 1320+4415†	M	53 ^b	2.76 ^c	3.78 ^b	3.08 ^b	<0.06	0.15 ^c	156 ^c	55 ^b	194 ^a
78	HS 1325+4823†	C	50 ^a	2.00 ^a	4.48 ^a	3.262 ^d	0.07 ^c	0.19 ^b	50 ^a	37 ^a	166 ^a
79	HS 1330+4351 [‡]	M	48 ^c				0.62 ^d		30 ^c		
80	HS 1331+3708*	B	18 ^d			4.33 ^d	0.28 ^c	0.44 ^c		5 ^d	

Table 5. (Continued)

#	Name	T	F(H β)	$\frac{F(3727)}{F(H\beta)}$	$\frac{F(5007)}{F(H\beta)}$	$\frac{F(H\alpha)}{F(H\beta)}$	$\frac{F(6583)}{F(H\alpha)}$	$\frac{F([SII])}{F(H\alpha)}$	EW ₃₇₂₇	EW _{Hβ}	EW ₅₀₀₇
	(2)	(3)	(4)	(5)	(6)	(7)	(8)	(9)	(10)	(11)	(12)
81	HS 1333+3522*†	B	10 ^d		4.72 ^d	6.52 ^d	<0.12	0.29 ^d		5 ^d	26 ^b
82	HS 1340+3806*	B	11 ^d		2.45 ^d	4.29 ^d	<0.16	0.36 ^c		8 ^d	20 ^c
83	HS 1340+4428	M	61 ^a	2.21 ^b	4.71 ^a	3.25 ^a	0.04 ^d	0.14 ^c	124 ^b	44 ^a	193 ^a
84	HS 1341+4318	M	29 ^a		6.07 ^a	3.26 ^a	0.04 ^d	0.12 ^d		122 ^a	622 ^a
85	HS 1353+4706	B	14 ^a	0.28 ^c	6.35 ^a	2.79 ^a	<0.03	0.01 ^d	55 ^c	223 ^a	1880 ^a
86	HS 1356+4159†	M	65 ^a	2.96 ^b	3.28 ^a	4.31 ^a	0.10 ^c	0.18 ^b	81 ^b	22 ^a	74 ^a
87	HS 1358+4447	M	18 ^c	4.56 ^c	2.67 ^c	3.65 ^c	0.13 ^d	0.35 ^c	103 ^c	20 ^c	49 ^a
88	HS 1407+3540*	B	41 ^b	2.97 ^b	3.80 ^b	4.12 ^b	<0.07	0.14 ^b	78 ^b	37 ^b	140 ^b
89	HS 1417+4011*	B	15 ^d	4.25 ^d	4.08 ^d	4.02 ^d	<0.10	0.23 ^d	42 ^c	10 ^d	43 ^b d
90	HS 1417+4027	M	13 ^c		3.02 ^c	3.91 ^c	0.12 ^d	0.27 ^d		28 ^c	87 ^a
91	HS 1423+4712	C	81 ^c		7.51 ^c	3.61 ^c	<0.09	0.25 ^d		27 ^c	245 ^a
92	HS 1424+3558*†	B	24 ^c	2.74 ^d	1.26 ^d	3.93 ^d	0.24 ^d	0.44 ^c	35 ^d	10 ^c	12 ^c
93	HS 1426+3658 [‡] *	C	44				0.20	0.46	14		7
94	HS 1437+3724 [‡]	C	1.2 ^d								
95	HS 1439+3704 [‡]	C	6.9 ^b				0.34 ^d	0.26 ^d			
96	HS 1510+5019†	B	53 ^a	1.42 ^a	2.44 ^a	3.41 ^a	0.13 ^b	0.13 ^b	161 ^a	63 ^a	158 ^a
97	HS 1525+4344 [‡]	C	148 ^b							50 ^c	4 ^d
98	HS 1536+4557*†	M	133 ^a	2.18 ^a	3.49 ^a	13.84 ^d	0.10 ^b	0.14 ^b	111 ^a	48 ^a	163 ^a
99	HS 1543+3602	B	8.4 ^a	1.29 ^b	5.61 ^a				55 ^b	37 ^a	214 ^a
100	HS 1545+4641	M	15.8 ^c	8.88 ^c	2.97 ^c	4.55 ^c	0.12 ^d	0.31 ^c	211 ^b	9 ^c	26 ^b
101	HS 1547+4421†	M	17.7 ^c		3.43 ^c	4.54 ^c	<0.55	0.42 ^d		7 ^c	25 ^a
102	HS 1605+4440	C	7.0 ^b	8.52 ^c	1.83 ^c	10.76 ^b	0.20 ^c	0.23 ^c	46 ^c	4 ^b	7 ^b
103	HS 1607+3621 [‡] *	C	35 ^a				0.16 ^c	0.59 ^c			5 ^b
104	HS 1613+3902†	B	12 ^c	2.53 ^c	5.07 ^c				36 ^c	10 ^c	49 ^b
105	HS 1614+4450 [‡]	C	11 ^b				0.27 ^d	0.28 ^c			
106	HS 1616+4023†	C	40 ^a		2.72 ^a	3.37 ^a	0.11 ^c	0.22 ^b		16 ^a	47 ^a
107	HS 1624+4143†	B	32 ^a	3.54 ^a	3.00 ^a				67 ^a	19 ^a	57 ^a
108	HS 1627+3625*	B	155 ^b		0.85 ^a	2.14 ^d	0.07 ^d	0.09 ^d		56 ^b	47 ^b
109	HS 1629+4513†	M	28 ^a	3.75 ^b	3.24 ^a	3.67 ^a	0.08 ^d	0.27 ^c	64 ^a	19 ^a	59 ^a
110	HS 1629+4820	M	14 ^c		4.99 ^c	4.22 ^c	<0.09	0.17 ^d		26 ^c	151 ^a
111	HS 1636+4319†	M	59 ^b	2.97 ^b	2.16 ^b	4.10 ^b	0.15 ^b	0.28 ^b	57 ^b	21 ^b	44 ^a
112	HS 1637+4206	M							85 ^d		
113	HS 1644+3934*	B	163 ^b		0.45 ^c	2.85 ^b	0.12 ^b			44 ^b	20 ^b
114	HS 1645+4211	M	45 ^b	2.94 ^c	3.66 ^b	4.09 ^b	0.09 ^c	0.21 ^c	61 ^c	23 ^b	81 ^a
115	HS 1645+3551	B	35 ^a	1.69 ^a	4.66 ^a				148 ^a	54 ^a	234 ^a
116	HS 1645+4401†	C	6.7 ^c		3.18 ^c	37.97 ^d	0.14 ^b	0.32 ^b		5 ^c	15 ^b
117	HS 1651+4933†	M	43 ^b	2.84 ^c	4.97 ^b	3.67 ^b	<0.06	0.16 ^c	112 ^c	22 ^b	106 ^a
118	HS 1700+4907†	M	37 ^b	3.27 ^c	2.48 ^b	4.53 ^b	0.09 ^d	0.39 ^b	56 ^c	16 ^b	38 ^a
119	HS 1702+4146†	C	40 ^a		1.71 ^a	3.80 ^a	0.14 ^b	0.27 ^a		16 ^a	28 ^a
120	HS 1711+3756	B	69 ^a	2.00 ^a	4.17 ^a				59 ^a	33 ^a	141 ^a

Table 5. (Continued)

#	Name	T	F(H β)	$\frac{F(3727)}{F(H\beta)}$	$\frac{F(5007)}{F(H\beta)}$	$\frac{F(H\alpha)}{F(H\beta)}$	$\frac{F(6583)}{F(H\alpha)}$	$\frac{F([SII])}{F(H\alpha)}$	EW ₃₇₂₇	EW _{Hβ}	EW ₅₀₀₇
	(2)	(3)	(4)	(5)	(6)	(7)	(8)	(9)	(10)	(11)	(12)
121	HS 1715+4827†	M	41 ^a	2.15 ^d	4.48 ^a	2.89 ^a	<0.06	0.11 ^d	374 ^d	69 ^a	235 ^a
122	HS 1720+4720	M	61 ^a	3.68 ^b	1.74 ^a	3.98 ^a	0.19 ^b	0.19 ^b	227 ^b	31 ^a	54 ^a
123	HS 1723+4410‡	M	16 ^c				0.27 ^d	0.52 ^d			
124	HS 1724+4001‡	M	22 ^a				0.32 ^d	0.50 ^d			
125	HS 1730+4601	M	105 ^a	0.59 ^c	6.52 ^a	3.16 ^a	<0.03	0.05 ^d	39 ^c	159 ^a	915 ^a
126	HS 1733+4035†	M	66 ^a	2.85 ^b	2.00 ^a	4.98 ^a	0.16 ^b	0.22 ^b	71 ^b	23 ^a	46 ^a

‡ No H β detected, the flux is given for H α ; * spectrum was acquired in non-photometric conditions.

† galaxy with the apparent underlying Balmer absorption. H β emission related parameters can be affected.

Letters ‘B’, ‘C’ and ‘M’ in Col. 3 are respectively for BTA, Calar Alto 2.2 m telescope and MMT.

¹ due to poor focus H α /H β ratio is too high; ² [N II] λ 6583/H α ratio is unreliable due to poor sky subtraction.

³ H α /H β ratio is unreliable due to poor sensitivity curve.

superscripts *a, b, c, d* for all entries denote class of relative error: <5%, (5–10)%, (10–20)% and (20–50)% respectively.

Table 6. Coordinates, redshifts and magnitudes of QSOs

#	Name	α (1950)	δ (1950)	z^a	m_B	Detected emission lines
	(2)	(3)	(4)	(5)	(6)	(7)
1	HS 1138+4900	11 38 13.4	+49 00 09	3.353	18.9	Ly α 1216 Å, SiIV/OIV] 1400 Å, CIV 1549 Å
2	HS 1203+3811	12 03 53.7	+38 11 09	3.184	+19.6	Ly α 1216 Å
3	HS 1250+4408	12 50 27.1	+44 08 53	1.639	+18.4	CIV 1549 Å, CIII] 1909 Å, MgII 2798 Å
4	HS 1334+3948	13 34 52.3	+39 48 15	3.223	19.1	Ly α 1216 Å, SiIV/OIV] 1400 Å, CIV 1549 Å
5	HS 1528+3914	15 28 39.4	+39 14 25	3.290	17.0	Ly α 1216 Å, SiIV/OIV] 1400
6	HS 1608+3546	16 08 00.5	+35 46 30	0.829	17.8	MgII 2798 Å
7	HS 1646+4501	16 46 19.0	+45 01 32	1.790	19.0	CIV 1549 Å, CIII] 1909 Å
8	HS 1714+4202	17 14 46.3	+42 02 49	0.846	+18.1	MgII 2798 Å

^a Observed redshift; + corrected APM magnitudes (see Sect. 4.2).

Table 7. Galaxies without detected emission lines

#	Name	α (1950)	δ (1950)	v_0^a	m_B	M_B^b	Absorption lines
	(2)	(3)	(4)	(5)	(6)	(7)	(8)
1	HS 0716+4510 [†]	07 16 35.8	+45 10 09	33994	19.2	-19.0	H α , NaD
2	HS 0805+4120 [†]	08 05 01.7	+41 20 23	17071	+17.8	-18.9	H β , H γ , G_{band} , CaK, CaH
3	HS 1010+4906 ¹	10 10 00.3	+49 06 56	18070	19.3	-17.6	CaK, CaH, G_{band} , MgIb, NaD, probable emis. H α
4	HS 1052+3637 [†]	10 52 32.9	+36 37 05	7774	19.0	-16.1	CaK, CaH
5	HS 1350+4701 [†]	13 50 52.3	+47 01 41	18570	17.7	-19.2	H α
6	HS 1420+4624 [†]	14 20 21.1	+46 24 39	9276	18.5	-16.9	H α , H β , MgIb
7	HS 1443+4253	14 43 07.8	+42 53 13	5082	+18.1	-16.1	CaK, CaH, H β , MgIb, TiO 6155-6180
8	HS 1454+3513	14 54 22.4	+35 13 30	35356	+19.1	-19.2	H α , H β , CaK, CaH, MgIb
9	HS 1527+4252 [†]	15 27 06.3	+42 52 55	35360	+17.5	-20.8	H α , H β , H γ , G_{band} ,

^a Heliocentric velocities; ^b absolute magnitudes are not corrected for galactic extinction;

[†] objects from the APM second priority sample; + APM magnitude.

¹ a galaxy near HS 1009+4906 and HS 1010+4907 in Table 4.

Table 8. Stars

#	Name	α (1950)	δ (1950)	m_B	Type	Spectral features
	(2)	(3)	(4)	(5)	(6)	(7)
1	HS 0712+4338 [‡]	07 12 46.4	+43 38 30	18.0	F-G	H α , H β , H γ , CaK, CaH
2	HS 0721+4148	07 21 16.0	+41 48 55	18.0	?	H α , NaD, CaK, CaH
3	HS 0729+4559 [‡]	07 29 08.8	+45 59 03	18.0	F-G	H α , NaD, H β , H γ
4	HS 0742+4205 [‡]	07 42 11.9	+42 05 38	17.9	F	H α , H β , H γ , CaK, CaH, NaD, MgIb
5	HS 1019+4002 [‡]	10 19 36.5	+40 02 20	17.2	G	CaK, CaH, G $_{band}$, H γ , H β , MgIb
6	HS 1027+4930	10 27 32.5	+49 30 33	19.0	K	CaK, CaH, G $_{band}$, FeI, MgIb, NaD
7	HS 1246+4514	12 46 12.1	+45 14 33	19.0	M	NaD, CaK, CaH, TiO-bands
8	HS 1317+4521A	13 17 49.6	+45 22 14	+17.3	K	CaK, CaH, G $_{band}$, FeI, H β , MgIb, NaD, H α
9	HS 1350+5022	13 50 14.6	+50 22 41	18.4	F	H α , H β , H γ
10	HS 1400+3833 [‡]	14 00 04.3	+38 33 22	18.7	K	CaK, CaH, G $_{band}$, FeI, MgIb, NaD
11	HS 1502+4358 [‡]	15 02 17.7	+43 58 57	+16.9	K	CaK, CaH, G $_{band}$, FeI, H β , MgIb, NaD, H α
12	HS 1514+4506 [‡]	15 14 29.8	+45 06 29	+17.6	G	CaK, CaH, G $_{band}$, H β , MgIb, NaD, H α
13	HS 1543+4919 [‡]	15 43 29.5	+49 19 07	19.2	A	H γ , H β , H α
14	HS 1609+4518 [‡]	16 09 47.0	+45 18 48	19.0	F	H γ , H β , NaD, H α
15	HS 1613+4408 [‡]	16 13 18.4	+44 08 07	17.8	F	H α , H β , H γ
16	HS 1614+4646 [‡]	16 14 22.7	+46 46 55	17.9	F-G	H α , H β , H γ , NaD
17	HS 1614+4835 [‡]	16 14 09.4	+48 35 20	18.0	A-F	H β , H γ , CaK, CaH
18	HS 1615+4512 [‡]	16 15 45.4	+45 12 09	17.6	F	H α , H β , H γ , CaK, CaH
19	HS 1647+4024 [‡]	16 47 31.7	+40 24 02	+17.1	A-F	H α , H β , H γ , G $_{band}$
20	HS 1654+3939 [‡]	16 54 53.2	+39 39 54	17.6	A	CaK, CaH, H γ , TiII, H β , H α
21	HS 1659+4059 [‡]	16 59 57.2	+40 59 36	+18.1	F	CaK, CaH, G $_{band}$, H β , MgIb, NaD, H α
22	HS 1703+4242 [‡]	17 03 02.4	+42 42 12	+18.0	A	H α , H β , H γ
23	HS 1720+4950 [‡]	17 20 10.9	+49 50 03	18.2	F-G	CaK, CaH, G $_{band}$, H β , MgIb, NaD, H α
24	HS 1721+4624 [‡]	17 21 41.7	+46 24 49	18.1	G	CaK, CaH, G $_{band}$, FeI, H β , MgIb, NaD, H α
25	HS 1722+4829 [‡]	17 22 51.4	+48 29 05	17.4	F-G	CaK, CaH, G $_{band}$, H β , MgIb, NaD, H α
26	HS 1733+4441 [‡]	17 33 59.5	+44 41 19	+16.8	F	CaK, CaH, H δ , G $_{band}$, H γ , H β , H α

[‡] objects from the APM selected sample; ⁺ APM magnitudes.